

Article

Modeling the Soil Erosion Regulation Ecosystem Services of the Landscape in Polish Catchments

Mustafa Nur Istanbuly ¹, Tomáš Dostál ² and Bahman Jabbarian Amiri ^{3,*}

¹ Department of Environmental Science, Faculty of Natural Resources, University of Tehran, Chamran Blvd., Karaj 31587-77878, Iran; istanbuly@ut.ac.ir

² Department of Landscape Water Conservation, Faculty of Civil Engineering, Czech Technical University in Prague, Thakurova 7, 16629 Prague, Czech Republic; dostal@fsv.cvut.cz

³ Department of Regional Economics and Environment, Faculty of Economics and Sociology, University of Lodz, 90-255 Lodz, Poland

* Correspondence: bahman.amiri@uni.lodz.pl

Abstract: In this study, the soil erosion regulation ecosystem services of the CORINE land use/land cover types along with soil intrinsic features and geomorphological factors were examined by using the soil erosion data of 327 catchments in Poland, with a mean area of $510 \pm 330 \text{ km}^2$, applying a multivariate regression modeling approach. The results showed that soil erosion is accelerated by the discontinuous urban fabric ($r = 0.224, p \leq 0.01$), by construction sites ($r = 0.141, p \leq 0.05$), non-irrigated arable land ($r = 0.237, p \leq 0.01$), and is mitigated by coniferous forest ($r = -0.322, p \leq 0.01$), the clay ratio ($r = -0.652, p \leq 0.01$), and the organic content of the soil ($r = -0.622, p \leq 0.01$). The models also indicated that there is a strong relationship between soil erosion and the percentage of land use/land cover types ($r^2 = [0.62, 0.82, 0.83, 0.74]$), i.e., mixed forest, non-irrigated arable land, fruit trees and berry plantations, broad-leaf forest, sport and leisure facilities, construction sites, and mineral extraction sites. The findings show that the soil erosion regulation ecosystem service is sensitive to broadleaf forests, rainfed agriculture, soil water content, terrain slope, drainage network density, annual precipitation, the clay ratio, the soil carbon content, and the degree of sensitivity increases from the broadleaf forest to the soil carbon content.

Keywords: regression models; Akaike information criterion; landscape composition; sensitivity analysis; goodness of fit tests



Citation: Istanbuly, M.N.; Dostál, T.; Jabbarian Amiri, B. Modeling the Soil Erosion Regulation Ecosystem Services of the Landscape in Polish Catchments. *Water* **2021**, *13*, 3274. <https://doi.org/10.3390/w13223274>

Academic Editor: Monica Papini

Received: 21 October 2021

Accepted: 15 November 2021

Published: 18 November 2021

Publisher's Note: MDPI stays neutral with regard to jurisdictional claims in published maps and institutional affiliations.



Copyright: © 2021 by the authors. Licensee MDPI, Basel, Switzerland. This article is an open access article distributed under the terms and conditions of the Creative Commons Attribution (CC BY) license (<https://creativecommons.org/licenses/by/4.0/>).

1. Introduction

Soil plays an essential role in the functioning of natural ecosystems [1]. Each soil ecosystem provides goods and services for the community, which can be called a soil ecosystem service [2]. Soil-based ecosystem services can be supportive (e.g., primary production, gene pool biodiversity, and habitat), regulatory (e.g., erosion control, water infiltration, water purification, nutrient retention, nutrient cycling, and pest control), and cultural (e.g., aesthetic) [1,3].

Soil ecosystem services depend on the properties of the soil and on their interactions [1]. The health of a soil ecosystem can therefore be determined from its physical, chemical and biological properties, e.g., activity level, stability, flexibility, and organization [2]. As a result, soil ecosystem services are more affected by land use/land cover, land management, and soil erosion [1]. The type and the quality of soil ecosystem services are related to the physical, chemical and biological characteristics of the soil, and these characteristics are influenced by various factors, such as soil erosion [4].

One of the strongest influencing factors on ecosystem services in general, and on soil systems in particular, is soil erosion [1,5]. Each year, about 36 to 75 billion tons of soil are eroded from the world's terrestrial ecosystems, and the result of soil erosion is the reduction in the overall productivity of terrestrial ecosystems [5,6].

Changes in land use/land cover and soil disruption have accelerated global soil erosion [6,7]. Land management and changes in land use/land cover affect the spatial patterns and the rate of accelerated soil erosion, and thus impact soil ecosystem services [6,8,9].

A comparison of the soil erosion generated by different land use/land covers indicates that there is a significant reduction in the amount of soil erosion when there is a change from arable land to semi-natural vegetation and to forests [6,9–11]. For example, Borrelli et al. [6] indicated that transforming forest land covers to another land use/to other land covers can potentially increase soil erosion by 0.61 billion tons yr^{-1} . Kogo et al. [9] showed that changing forest land cover to agricultural land use increased the amount of soil erosion rate from 0.43 ($\text{t ha}^{-1} \text{yr}^{-1}$) to 0.84 ($\text{t ha}^{-1} \text{yr}^{-1}$).

Depending on the composition, structure and configuration that they have in catchments, land use/land covers can accelerate and/or mitigate soil erosion. One of the most important ecosystem services provided by different land use/land covers is mitigation of soil erosion, and this also affects soil ecosystem services [4].

Xiong et al. [8] showed that bare lands can be considered as the land cover with the highest rate of soil erosion (10.6–109.2 $\text{t ha}^{-1} \text{yr}^{-1}$). Croplands have the second-highest rate of soil erosion (3.9–41.8 $\text{t ha}^{-1} \text{yr}^{-1}$), while forests (0.2–0.6 $\text{t ha}^{-1} \text{yr}^{-1}$) are the land cover with the lowest rate of soil erosion. The rate of soil erosion in orchards (23.52 $\text{t ha}^{-1} \text{yr}^{-1}$), in grasslands (0.3–3.62 $\text{t ha}^{-1} \text{yr}^{-1}$), and in shrublands (0.3–1.57 $\text{t ha}^{-1} \text{yr}^{-1}$), fall between the rates for bare lands and for forests, and can be arranged in descending order. Forest cover, both natural and artificial, is one of the most important land covers for providing protection against soil erosion [6,9,10,12].

Steinhoff-Knopp and Burkhard [13] indicated that the soil erosion rate for agricultural land use is highly dependent on the type of crop that is grown. They reported that root crops can increase soil erosion rates to 2.98 $\text{t ha}^{-1} \text{yr}^{-1}$ in the land where they are grown, due to intensive soil operations during planting and harvesting times. However, the soil erosion rates for fast-growing crops can be reduced to 0.07 $\text{t ha}^{-1} \text{yr}^{-1}$, mainly because of the reduced soil operation intensity during planting and harvesting times.

Agricultural land management, crop selection, and tillage management have significant impacts on soil loss rates [4,10,13,14]. Crops such as cereals, oilseeds and maize [4], and potatoes [13] are the agricultural products associated with the highest soil erosion rates, due to great amounts of tillage and the removal of crop residues of these crops [4].

When addressing soil erosion and the soil erosion regulation ecosystem service, it is necessary to take into account other exogenous and endogenous factors that affect the soil erosion process and thus change the quality and the quantity of the soil erosion mitigation ecosystem service.

The endogenous factors that affect the soil erosion process and the soil erosion mitigation ecosystem service originate from the intrinsic properties of the soil, e.g., the clay ratio [15], the soil organic carbon content [16] and the soil water content [17]. To be more specific, the organic carbon content in the soil has a mulching function, protecting the soil and increasing its resistance to erosion [16]. The soil water content increases the resistance of soil particles to the forces of raindrops and water flow, thus reducing the forces required to separate soil particles [18].

Climate factors [16,19,20], terrain slope, stream gradient, drainage density, and the physical characteristics of the catchment [16,21] can be considered as the main exogenous factors affecting the soil erosion process and the soil erosion regulation ecosystem service. Oguchi [22] studied the relationship between drainage density and soil erosion, as the density of the drainage network can determine the degree of resistance of rocks to erosion and the degree of permeability of the substrate.

Singh and Singh [23] showed that runoff is drained more efficiently in a circular catchment than in an elongated catchment. The morphometrical characteristics of catchments are therefore another group of factors that affect the response of the soil system, including soil erosion. The shape of the catchment can affect the drainage velocity of the runoff, thus affecting the amounts of soil erosion at catchment scale.

Few studies, if any, have addressed the three affecting factors together, e.g., land use/land covers, intrinsic features of soil, and geomorphological factors, in order to determine the contribution of these factors to accelerating and or mitigating soil erosion. The study presented here aims to fill this gap. The objectives of the study are (1) to investigate the role played by the Corine land use/landcover types in the soil erosion process, or, more specifically, to determine which types accelerate the soil erosion process, and which types mitigate soil erosion at catchment scale, and (2) to investigate the extent to which the intrinsic features of the soil, geomorphological factors, the catchment morphometrical factor, and climate factors, along with the type of land use/land cover, are important in accelerating and or mitigating soil erosion.

2. Materials and Methods

2.1. Study Area

The study area consists of 327 medium-sized catchments located in Poland ranging in area between 60 km² and 1338 km². These catchments are distributed in elevation between -1 m and 658 m a.s.l., terrain slope 23 ± 133%, annual precipitation 581 ± 53 mm yr⁻¹, and stream gradient 20 ± 60 decimeters per km. The most dominant land use/land cover type is non-irrigated arable land (42.7%), followed by coniferous forest (19.1%), pastures (8.7%), mixed forest (7.40%), broad-leaf forest (4.55%), and discontinuous urban fabric (4.99%) (Figure 1).

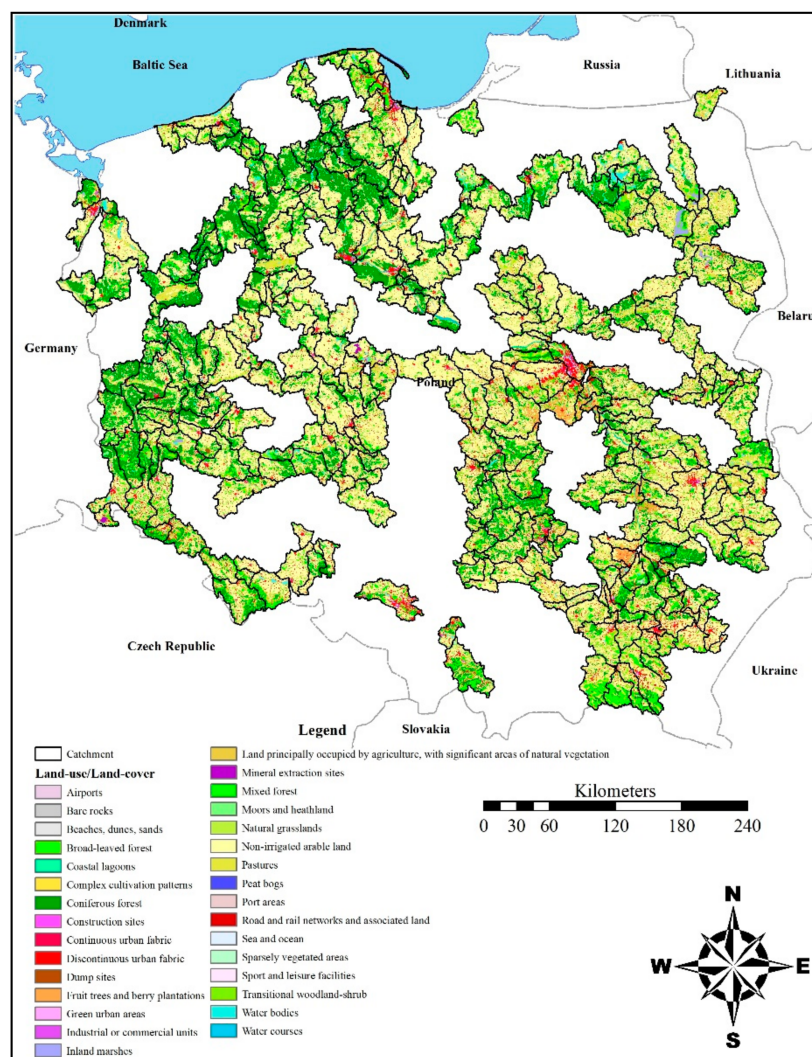


Figure 1. The geographical position of the study catchments and land use/land covers.

2.2. Data

To conduct this study, secondary data [24] were applied. The digital map of land use/land cover was acquired from the European Union's Earth Observation Program for year 2012. The map covers the EEA members with better than 100 m positional accuracy and with a 25 ha minimum mapping unit. The spatial resolution of the raster map is 100 m [25]. The digital maps of the study catchments, the terrain slope (deg.), the river networks (m km^{-1}), the stream gradient (dm km^{-1}), the organic content of the soil ($\text{t ha}^{-1} \text{yr}^{-1}$), the soil texture, the soil water content (%), and the soil erosion ($\text{kg ha}^{-1} \text{yr}^{-1}$) were obtained from [26] as the source of dataset for the present study.

2.3. Methods

The spatial data were obtained from various sources. They were transformed into a common digital format, then co-registered with ETRS89_Poland_CS92. To select more homogeneous catchments for the purposes of this study, we removed catchments with an area outside the range of $(+\delta > \mu > -\delta)$, where δ stands for standard deviation and μ is the average area of the catchment. The Corine land use/land cover map (2012) was overlaid by the digital map of the catchments in order to calculate the area percentage of land use/land cover types.

The clay ratio [16] was calculated by the sum of the percentage of sand and silt divided by the percentage of clay. The drainage density [27] was obtained by dividing the total length of all the streams by the area of the catchment.

Four variables related to the physical shape of a catchment, consisting of the compactness coefficient (K), the form coefficient (F), the elongation coefficient, and the circularity ratio [23,28–31], were calculated applying Equations (1)–(4), as follows:

$$K = 0.282 \frac{P}{\sqrt{A_c}} \quad (1)$$

$$F = \frac{A}{Lb^2} \quad (2)$$

$$E = \frac{D}{L_m} \quad (3)$$

$$C = \frac{A}{P_c} \quad (4)$$

where P is the perimeter of the catchment, A_c is the area of a circumscribing circle, A is the area of the catchment, Lb is the square of the catchment length, D is the diameter of the circle of the catchment area, L_m is the maximum length of the catchment and P_c is the area of a circle with the same circumference as the perimeter (P) of the catchment.

In order to tackle the issue of the large number of data items with a zero value in the dataset, a positive constant was added to the observations [32] to prepare the data for modeling purposes.

2.3.1. Modeling

A step-by-step regression model was applied in order to model the relationship between soil erosion as dependent variable and intrinsic variables of the soil, geomorphological variables and land use/land covers as independent variables. Four linear, power, logarithmic and exponential structures [33] were examined to determine which of these model structures could best explain the relationship between soil erosion and three explanatory factors: the intrinsic variables of the soil, the geomorphological variables, and land use/land covers.

To ascertain whether the models have any collinearity issues, variation inflation factors were calculated for each of the model parameters [34,35]. The goodness-of-fit (Figure 2) was evaluated by plotting the observed values versus the predicted values for soil erosion prediction models [36].

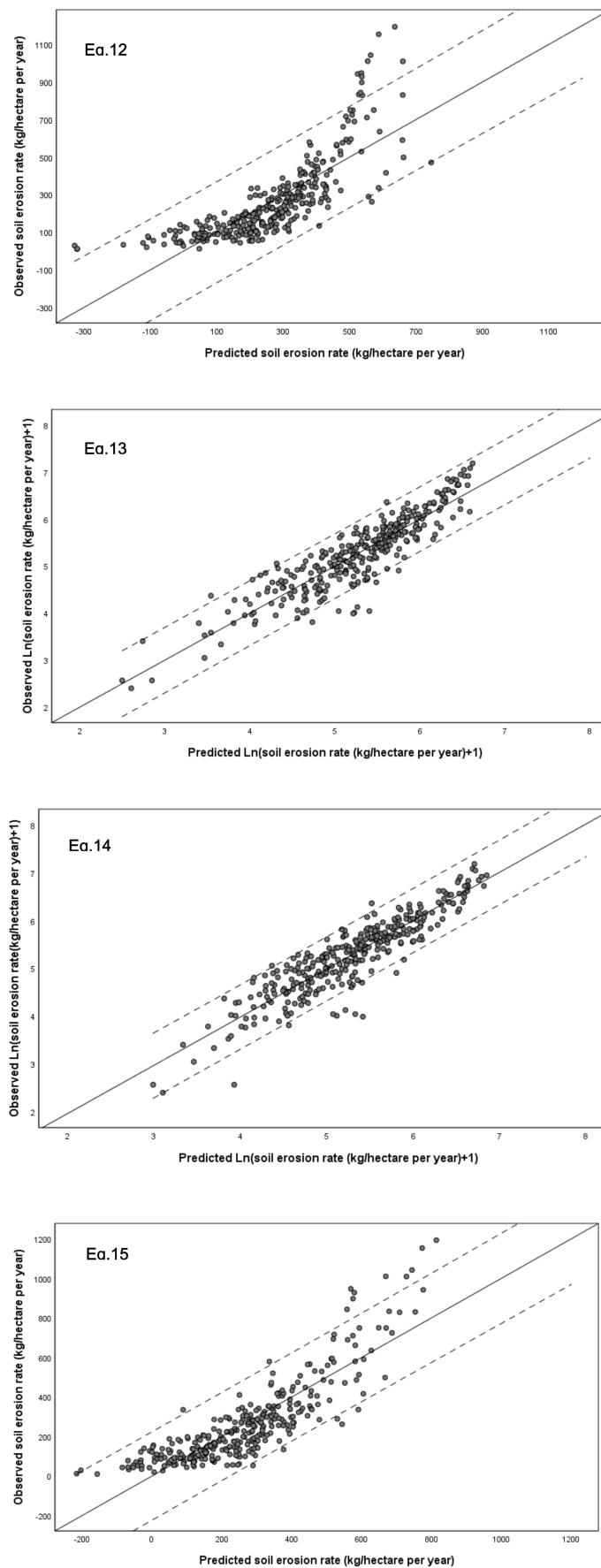


Figure 2. One-to-one diagrams for predicted values versus observed values.

To assess the validity of the models, the one-by-one plots of models were depicted and the validation metrics were calculated. The validation metrics include the relative absolute error, the absolute mean relative error, the absolute mean error percentage measurement, the relative mean, the relative square mean error value and the relative volumetric error (Table 1). All statistical analyses and landscape metrics calculations were conducted using IBM SPSS for Windows, Release 26, and Fragstat version 4.

Table 1. Validation metrics for assessing the validity of the models.

Metrics	Formula to Calculating Metrics	Equation No.	References	Results Means
Relative absolute error	$RAE = \frac{\sum_{i=1}^n O_i - P_i }{\sum_{i=1}^n O_i - \bar{O} }$	(5)		
Absolute mean relative error	$MARE = \frac{1}{n} \sum_{i=1}^n \frac{ O_i - P_i }{O_i}$	(6)		
Absolute mean error percentage	$MdAPE = Median\left(\left \frac{O_i - P_i}{O_i}\right \times 100\right)$	(7)	[37,38]	the closer the value to zero, the more appropriate the model
Relative mean	$MRE = \frac{1}{n} \sum_{i=1}^n \left(\frac{O_i - P_i}{O_i}\right)$	(8)		
Square mean error measure	$MSRE = \frac{1}{n} \sum_{i=1}^n \left(\frac{O_i - P_i}{O_i}\right)^2$	(9)		
Relative volumetric error	$RVE = \frac{\sum_{i=1}^n (O_i - P_i)}{\sum_{i=1}^n O_i}$	(10)		

Where; O_i : observation values; P_i : predicted values; \bar{O} : Mean of observation values.

2.3.2. Inter-Model Comparison

The most appropriate model was selected by applying the Akaike information criterion (AIC). This criterion shows the relationship between the Kulbakk-Leibner data loss index and the (numerical value) maximum likelihood. The maximum likelihood has been the estimation method used in many statistical analyses [37,39]. The numerical value of the Akaike information criterion is obtained from Equation (11) [37,40].

$$AIC_c = n \left(\log \frac{RSS}{n} \right) + 2K + \left(\frac{2K(K+1)}{n-K-1} \right) \quad (11)$$

where AIC_c is the value of the Akaike information criterion, RSS is the residual sum of squares, K is the number of model variables, including the distance variable from the origin of the model, and n the number of samples (observed or measured).

2.3.3. Sensitivity Analysis

The sensitivity analysis (SA) of models are an important step in improving models in general and environmental models in particular [37]. It aims to determine the extent to which the responses of a given model are sensitive to a change in the variables. Conditional SA was applied to analyze the sensitivity of the models. For this purpose, the outputs of the models were examined by changing the value of the variable of interest, while fixing the remaining variables to the mean. The outputs of the models were then depicted versus the incremental values in the variable of interest.

3. Results and Discussion

3.1. Result of Bivariate Analysis

The Pearson correlation test ($p \leq 0.05$ and $p \leq 0.01$ for $n = 327$) examined whether there is a significant relationship between the soil erosion rates and the Corine land use/land cover types, the intrinsic factors of the soil, and the geomorphological features at catchment scale. The results indicated (Table 2) that among the Corine land use/land cover types, there are five land use/land covers that correlate positively with the soil erosion rate. These covers are discontinuous urban fabric ($r = 0.224$, $p \leq 0.01$), construction sites ($r = 0.141$, $p \leq 0.05$), non-irrigated arable land ($r = 0.237$, $p \leq 0.01$), land principally occupied by

agriculture, with significant areas of natural vegetation ($r = 0.147, p \leq 0.01$), and complex cultivation patterns ($r = 0.247, p \leq 0.01$). This implies that increasing the area proportion of these land use/land cover types is significantly associated with an increase in the soil erosion rate in the study catchments, while coniferous forest ($r = 0.322, p \leq 0.01$) showed an inverse relationship with the soil erosion rate. Table 2 shows the results of the bivariate relationship analysis between the soil erosion rate, the Corine land use/land covers, intrinsic features of the soil, and geomorphological indicators.

Table 2. Pearson correlation test ($p \leq 0.05$ and $p \leq 0.01$ for $n = 327$) for the relationship between the soil erosion rates and the Corine land use/land cover types, soil intrinsic factors, and geomorphological features at catchment scale.

Type of Variable	Factors	Correlation Coefficient
Corine Land Use/Land Covers	Discontinuous urban fabric	0.224 **
	Construction sites	0.141 *
	Non-irrigated arable land	0.237 **
	Complex cultivation patterns	0.274 **
	Land principally occupied by agriculture, with significant areas of natural vegetation	0.147 **
	Coniferous forest	−0.322 **
Geomorphological factors	Terrain slope	0.277 **
	Compactness coefficient	−0.160 **
	Circularity ratio	0.143 **
	Clay ratio	−0.652 **
	Soil organic content	−0.622 **
Climate factors	Annual precipitation	0.155 **

** . Correlation is significant at the 0.01 level. * . Correlation is significant at the 0.05 level.

Both the clay ratio ($r = 0.652, p \leq 0.01$) and the organic content of the soil ($r = 0.622, p \leq 0.01$), which are intrinsic features of the soil, revealed a negative association with the soil erosion rate, as an increase in the values for the clay ratio and for the organic content of the soil are significantly associated with a decrease in the soil erosion rate.

Annual precipitation showed direct low correlation with soil erosion ($r = 0.155, p \leq 0.01$). Although the precipitation is an important factor and the main cause of soil erosion, other factors like the type of precipitation, the patterns of precipitation, and other factors may affect the relationship between precipitation and soil erosion [16,41–43].

3.2. Result of Modeling

Four regression model structures—linear, exponential, logarithmic, and power—were fitted using a step-by-step approach, applying land use/land cover, soil intrinsic factors (organic carbon content in soil, soil water content, clay ratio), geomorphological factors (terrain slope, stream gradient, drainage density, circularity ratio, elongation and form coefficient, compactness coefficients), along with the annual precipitation as independent variables and soil erosion as a dependent variable.

Equations (12)–(15), as follows, show that soil erosion can be explained by a set of independent variables.

$$E = 386.020 - 18.769(CR) - 9.083(SOC) + 6.050 (Slp) - 0.456(Sgr) + 0.664(Pre) - 5.325 (Clc19) \tag{12}$$

$$\begin{aligned} \ln(E + 1) = 6.994 - 0.032(SOC) - 0.110(CR) + 0.014(Slp) + 0.003(Clc12) + 0.003(Pre) - 0.012(Clc19) - \\ 0.842(DN) - 0.016(SWC) - 0.010(Clc13) \end{aligned} \tag{13}$$

$$\begin{aligned} \ln(E + 1) = 7.407 - 1.222\ln(CR + 1) - 1.330\ln(SOC + 1) + 0.228\ln(Slp + 1) - 1.798\ln(DN + 1) + \\ 0.093\ln(Clc12 + 1) - 0.076\ln(Clc17 + 1) + 1.698\ln(Pre + 1) - 1.333\ln(SWC + 1) \end{aligned} \tag{14}$$

$$\begin{aligned} E = 2003.977 - 217.833\ln(CR + 1) - 411.743\ln(SOC + 1) + 188.831\ln(Slp + 1) - 49.246\ln(Sgr + 1) - \\ 80.805\ln(Clc11 + 1) + 115.323\ln(Clc9 + 1) - 67.790\ln(Clc7 + 1) - 16.192\ln(Clc18 + 1) \end{aligned} \tag{15}$$

where, *E*: soil erosion, *CR*: clay ratio, *SOC*: soil organic carbon content, *SWC*: soil water content, *Slp*: terrain slope, *Sgr*: stream gradient, *DN*: drainage network density, *Pre*: precipitation, *Clc7*: mineral extraction sites, *Clc9*: construction sites, *Clc11*: sport and leisure facilities, *Clc12*: non-irrigated arable land, *Clc13*: fruit trees and berry plantations, *Clc17*: broad-leaf forest, *Clc18*: coniferous forest, and *Clc19*: mixed forest.

Equations (12)–(15) show that only eight out of the 31 Corine land use/land cover types entered the models based on a step-by-step approach. Models (12 to 15) have varying coefficients of determination (0.62, 0.82, 0.83, 0.73), respectively. They also indicate that there is a relationship between soil erosion and the percentage of land use/land cover types: mixed forest, non-irrigated arable land, fruit trees and berry plantations, broad-leaf forest, sport and leisure facilities, construction sites, and mineral extraction sites.

In addition, all the soil-related variables—clay ratio, soil organic carbon content and soil water content—entered the models. The clay ratio correlates negatively with soil erosion, i.e., the higher the clay ratio, the lower the soil erosion. The negative relationship between the clay ratio and soil erosion is not consistent with the findings of Bouyoucos [15], who reported that the higher the clay ratio, the greater the soil erosion. Bouyoucos [15] and Egashira et al. [44] showed that the relationship between the clay ratio and soil erosion can be region-specific and dependent on soil types.

Sand and silt particles have high erosion potential, and soil erosion can increase if the percentage of these particles in the soil increases. An increase in the percentage of clay increases the adhesion of soil particles and thus increases the resistance of the soil to erosion. This implies that a decrease in the value of the clay ratio is associated with a decrease in the soil erosion value, because there is an increased percentage of clay in the soil texture.

The negative relationship between the clay ratio and soil erosion is consistent with the findings of Egashira et al. [44], who observed a negative relationship between the clay ratio and soil erosion in granitic soils in the southern part of Japan, which varied from place to place.

The soil organic carbon content in all of the models correlated negatively with soil erosion, i.e., soil erosion will increase if the organic carbon content of the soil decreases. Morgan [16] emphasized increasing the organic carbon content of soil to combat soil erosion. The role played by the soil organic matter depends on its origin, but the organic matter acts as a mulch to protect the soil and increase its resistance to erosion [16].

In models 12 to 14, annual precipitation correlated positively with soil erosion, and the greater the amount of annual precipitation, the higher the soil erosion value. Rainfall is the main cause of soil loss. Rainfall is a prerequisite for runoff and for soil water erosion, and the amount of soil erosion and runoff is determined by the amount of rainfall [16,41].

The terrain slope, one of the geomorphological features of a catchment, correlates positively with soil erosion, i.e., soil erosion will increase with an increasing terrain slope value.

The density of the drainage network entered models 13 and 14. It correlated negatively with soil erosion. That is, if there is an increase in the density of the drainage network, the soil erosion value will decrease across the catchments. The relationships between soil erosion and drainage network density vary depending on the slope threshold of the dominant hill [45]. This means that the greater the density of the drainage network, the lower the soil erosion rates will be at catchment scale.

Clubb et al. [46] indicated the relationship between drainage density and erosion rate by applying the model of Channel-Hillslope Integrated Landscape Development. They showed that there is an indirect relationship between drainage network density and soil erosion.

This can be related to runoff velocity and other factors. If soil reaction velocity to rainwater is low, the runoff will be directed into the drainage network and the soil erosion rates will be reduced in various parts of the catchments [45].

Clubb et al. [46] found that there is a significant relationship between soil erosion values and the terrain slope and some other fluvial morphological controls, while Oguchi [22] found that the relationship between drainage density and soil erosion can be region-specific.

Soil water content (Equations (13) and (14)) correlates negatively with the soil erosion value, i.e., the amount of soil erosion decreases with an increase in the percentage of soil water content. Increasing the initial state of water in the soil increases the resistance of soil particles (total aggregate stability) to the forces of raindrops and water flow, thus reducing the forces required for separating soil particles [17,18].

The stream gradient entered into the all model structure (12 and 15) through the stepwise regression modeling approach. The stream gradient correlates negatively with soil erosion, i.e., when the stream gradient in the catchments decreases, the erosion value increases at catchment scale. Likewise, the soil erosion rate decreases with an increase in the terrain slope gradient. Liu et al. [47] showed that the critical slope gradient for soil erosion is dependent on grain size, soil bulk density, surface roughness, runoff length, net rain excess, and the friction coefficient. The critical slope gradient has been estimated theoretically, ranging between 41.5–50°. The findings of Liu et al. [47] revealed that soil erosion increases when there is an increase in the runoff velocity, but after passing the threshold (the critical slope gradient), the soil erosion starts to decrease as the slope gradient increases.

3.3. Results of a Goodness-of-Fit Test

An evaluation of the goodness-of-fit of the models (Equations (12)–(15)) was conducted by referring to the values of the coefficient of determination, the significance of the models, and their coefficients at a level of $p \leq 0.05$. Figure 2 shows one-to-one diagrams for the predicted values versus the observed values.

The appropriate model for explaining soil erosion using validation metrics (RAE, MARE, and MdAPE) is Equation (14), while for the values of validation metrics (MRE, MSRE, and RVE), the most appropriate model is model 13.

Conducting an inter-modal comparison could provide more reliability in the choice of the most appropriate model, since it is confusing to rely only on the values of the validation metrics while deciding on the most appropriate model, and validation metrics gave two choices.

3.4. Results of the Inter-Modal Comparison

To select the most appropriate model from among the models that have been developed, an inter-modal comparison was conducted applying the Akaike Information Criterion. The comparison among the models shows that Equation (14) is the most appropriate model, with the lower AIC value, for obtaining a relatively close approximation of the soil erosion process. Table 3 provides more details about the inter-model comparison.

Table 3. Results of the inter-model comparison using the Akaike Information Criteria for soil erosion regression models using the landscape PLAND metric.

Model No.	RSS	n	log(RSS/n)	K	2 K	K + 1	n – K – 1	AIC	Δ_j	EXP(–0.5 * Δ_j)	Wi
12	440.3181	327	1.0640	7	14	8	319	362.2735	344.6866	1.42×10^{-75}	1.40×10^{-75}
13	39.5669	327	0.0175	10	20	11	316	26.4344	8.8474	1.20×10^{-2}	1.18×10^{-2}
14 *	37.7384	327	–0.0030	9	18	10	317	17.5870	0.0000	1.00×10^0	9.88×10^{-1}
15	439.9875	327	1.0637	9	18	10	317	366.3836	348.7966	1.82×10^{-76}	1.80×10^{-76}

* The most appropriate model.

3.5. Results of a Sensitivity Analysis

The results of a sensitivity analysis (Figure 3) showed that the first and second important variables that contribute to soil erosion are the soil organic carbon content and the clay ratio, while soil erosion shows the least sensitivity to a change in the percentage values of the broad-leaf forest and non-irrigated arable land. Annual precipitation can also be

ranked as the third important factor contributing to the sensitivity of soil erosion to the change in the value.

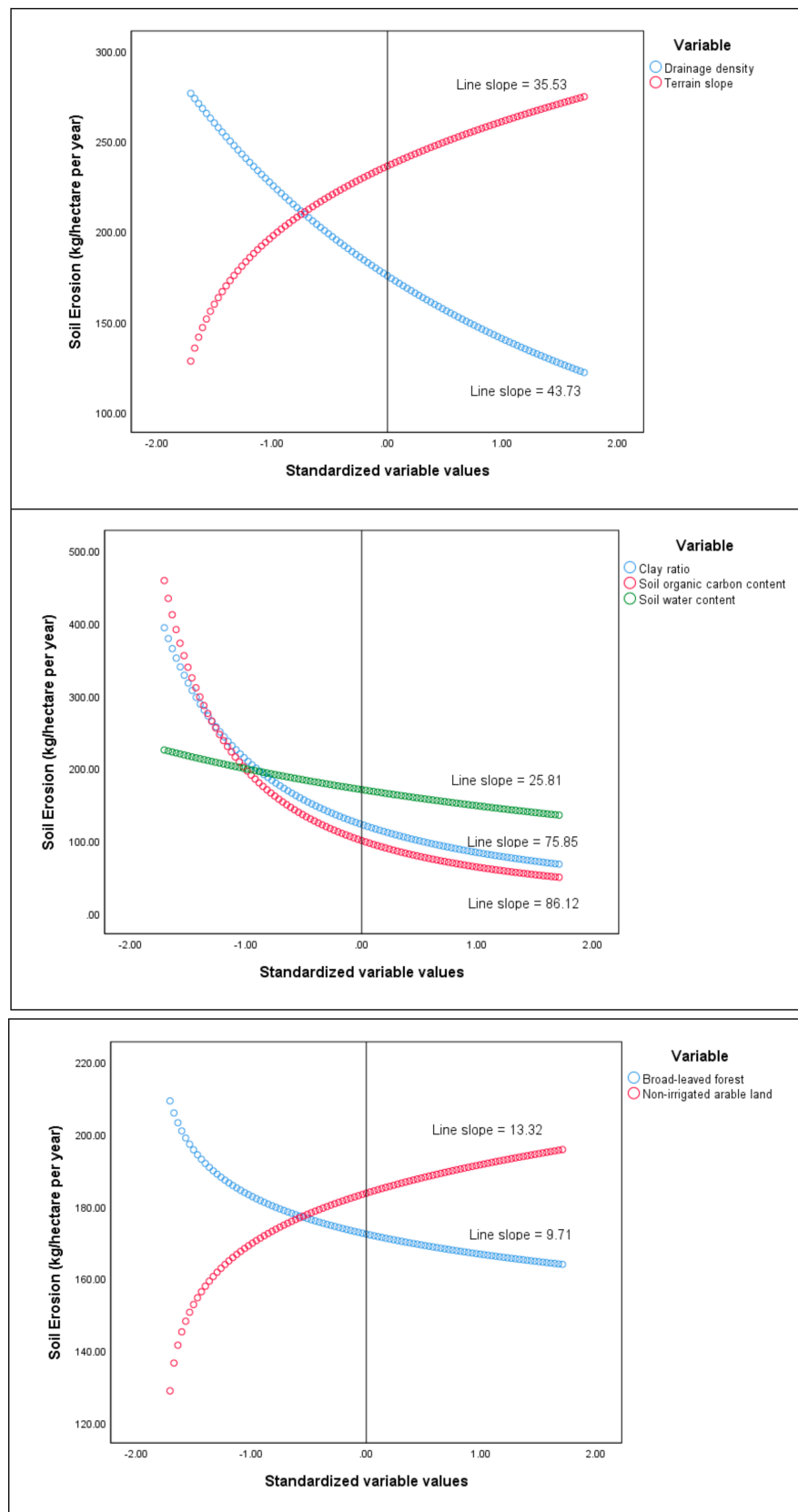


Figure 3. Results of the sensitivity analysis.

4. Conclusions

This study has shown that out of thirty-one Corine land use/land cover types, three man-made land-use types (mineral extraction sites, construction sites, sport and leisure facilities); two semi-natural land cover types (non-irrigated arable land, and fruit trees and berry plantations); and three natural land cover types (broad-leaf forest, coniferous forest, and mixed forest) can be observed in the models that have been developed, and can be used as key land use/land cover types in determining and managing soil erosion at catchment scale.

The results of the study indicate that the Corine land use/land cover can be categorized in the viewpoint of providing soil erosion control services into two groups: (a) the soil erosion-mitigating land use/land cover, which includes broad-leaf forest, coniferous forest, and mixed forest as natural types of land cover, fruit trees and berry plantations as semi-natural land cover types, mineral extraction sites, and sport and leisure facilities as man-made land uses, and (b) the soil erosion-elevating land use/land cover, which includes non-irrigated arable land as a semi-natural land cover, and construction sites as man-made land use.

According to the findings, man-made land-use types (mineral extraction sites, construction sites, sport and leisure facilities) and mineral extraction sites along with sport and leisure facilities reduce soil erosion, while construction sites raise the level of soil erosion at catchment scale. This is because the surface of the soil is disturbed by removing the vegetation cover and by construction operations. Natural land cover types (broad-leaf forest, coniferous forest and mixed forest) provide varying degrees of soil erosion mitigation as services to the ecosystem.

Among the semi-natural land cover types, non-irrigated arable land causes an increase in soil erosion values due to annual agricultural practices and because the land is uncovered for a part of the year. However, fruit trees and berry plantations mitigate soil erosion at catchment scale, because there is permanent vegetation cover.

It should be noted that the results presented in this study can be considered as scale-specific findings, considering that the resolutions of the land use/land cover map and the soil erosion map are 250 and 100 m, respectively. The findings can therefore be in the exposure of change due to change in the resolution of the information layers which are applied to conduct it.

Author Contributions: Supervision, B.J.A., T.D.; Writing—original draft, M.N.I.; Writing—review and editing, B.J.A., M.N.I., T.D. All authors have read and agreed to the published version of the manuscript.

Funding: This research received no external funding.

Institutional Review Board Statement: Not applicable.

Informed Consent Statement: Not applicable.

Data Availability Statement: Available upon request.

Acknowledgments: This manuscript has been issued within the framework of project H2020 SHUi, No. 773903, focused on water scarcity in European and Chinese cropping systems.

Conflicts of Interest: The authors declare no conflict of interest.

References

1. Adhikari, K.; Hartemink, A.E. Linking soils to ecosystem services—A global review. *Geoderma* **2016**, *262*, 101–111. [[CrossRef](#)]
2. Faber, J.H.; van der Pol, J.J.C.; Rutgers, M. Soil quality and ecosystem services: A land use perspective. In *Multiple Stressors for the Environment and Human Health, Present and Future Challenges and Perspectives*; book of abstracts book; SETAC Europe 17th annual meeting; SETAC: Porto, Portugal, 2007; p. 243.
3. Baer, S.G.; Birgé, H.E. Soil ecosystem services: An overview. *Manag. Soil Health Sustain. Agric.* **2018**, *1*, 17–38. [[CrossRef](#)]
4. Rendon, P.; Steinhoff-Knopp, B.; Saggau, P.; Burkhard, B. Assessment of the relationships between agroecosystem condition and the ecosystem service soil erosion regulation in Northern Germany. *PLoS ONE* **2020**, *15*, e0234288. [[CrossRef](#)] [[PubMed](#)]

5. Pimentel, D.; Kounang, N. Ecology of Soil Erosion in Ecosystems. *Ecosystems* **1998**, *1*, 416–426. Available online: <http://www.jstor.org/stable/3658674> (accessed on 8 March 2021). [[CrossRef](#)]
6. Borrelli, P.; Robinson, D.A.; Fleischer, L.R.; Lugato, E.; Ballabio, C.; Alewell, C.; Meusburger, K.; Modugno, S.; Schütt, B.; Ferro, V.; et al. An assessment of the global impact of 21st century land use change on soil erosion. *Nat. Commun.* **2017**, *8*, 1–13. [[CrossRef](#)]
7. Walling, D.E. Linking land use, erosion and sediment yields in river basins. *Hydrobiologia* **1999**, *410*, 223–240. [[CrossRef](#)]
8. Xiong, M.; Sun, R.; Chen, L. A global comparison of soil erosion associated with land use and climate type. *Geoderma* **2019**, *343*, 31–39. [[CrossRef](#)]
9. Kogo, B.; Kumar, L.; Koech, R. Impact of Land Use/Cover Changes on Soil Erosion in Western Kenya. *Sustainability* **2020**, *12*, 9740. [[CrossRef](#)]
10. Yin, Z.; Zuo, C.; Ma, L. Soil Erosion Features by Land Use and Land Cover in Hilly Agricultural Watersheds in Central Sichuan Province, China. In *Computer and Computing Technologies in Agriculture IV*; Li, D., Liu, Y., Chen, Y., Eds.; IFIP Advances in Information and Communication Technology; Springer: Berlin/Heidelberg, Germany, 2011; Volume 345, pp. 538–550.
11. Fu, B.; Liu, Y.; Lü, Y.; He, C.; Zeng, Y.; Wu, B. Assessing the soil erosion control service of ecosystems change in the Loess Plateau of China. *Ecol. Complex.* **2011**, *8*, 284–293. [[CrossRef](#)]
12. Wijitkosum, S. Impacts of land use changes on soil erosion in Pa Deng sub-district, adjacent area of Kaeng Krachan National Park, Thailand. *Soil Water Res.* **2012**, *7*, 10–17. [[CrossRef](#)]
13. Steinhoff-Knopp, B.; Burkhard, B. Soil erosion by water in Northern Germany: Long-term monitoring results from Lower Saxony. *Catena* **2018**, *165*, 299–309. [[CrossRef](#)]
14. Myronidis, D.; Ioannou, D.; Sapountzis, M.; Fotakis, D. Development of a sustainable plan to combat erosion for an island of the Mediterranean region. *Fresenius Environ. Bull.* **2010**, *19*, 1694–1702.
15. Bouyoucos, G.J. The Clay Ratio as a Criterion of Susceptibility of Soils to Erosion 1. *Agron. J.* **1935**, *27*, 738–741. [[CrossRef](#)]
16. Webster, R.; Morgan, R.P.C. *Soil Erosion and Conservation*, 3rd ed.; Blackwell Publishing: Oxford, UK, 2005; ISBN 1-4051-1781-8. [[CrossRef](#)]
17. Truman, C.C.; Bradford, J.M.; Ferris, J.E. Antecedent Water Content and Rainfall Energy Influence on Soil Aggregate Breakdown. *Soil Sci. Soc. Am. J.* **1990**, *54*, 1385–1392. [[CrossRef](#)]
18. Martínez-Mena, M.; Williams, A.; Ternan, J.; Fitzjohn, C. Role of antecedent soil water content on aggregates stability in a semi-arid environment. *Soil Tillage Res.* **1998**, *48*, 71–80. [[CrossRef](#)]
19. Milliman, J.D.; Farnsworth, K.L. *River Discharge to the Coastal Ocean: A Global Synthesis*; Cambridge University Press: New York, NY, USA, 2011; pp. 316–323.
20. Li, T.; Dong, J.; Yuan, W. Effects of Precipitation and Vegetation Cover on Annual Runoff and Sediment Yield in Northeast China: A Preliminary Analysis. *Water Resour.* **2020**, *47*, 491–505. [[CrossRef](#)]
21. Chapter 3 Erosion Factors. In *Developments in Soil Science*; Dvořák, J.; Novák, L. (Eds.) Elsevier: Amsterdam, The Netherlands, 1994; Volume 23, pp. 39–80. ISBN 9780444987921. [[CrossRef](#)]
22. Oguchi, T. Drainage Density and Relative Relief in Humid Steep Mountains with Frequent Slope Failure. *Earth Surf. Process. Landforms.* **1997**, *22*, 107–120. [[CrossRef](#)]
23. Singh, S.; Singh, M.C. Morphometric analysis of Kanhar River Basin. *Natl. Geogr. J. India.* **1997**, *43*, 31–43.
24. Amiri, B.J.; Gao, J.; Fohrer, N.; Adamowski, J.; Huang, J. Examining lag time using the landscape, pedoscape and lithoscape metrics of catchments. *Ecol. Indic.* **2019**, *105*, 36–46. [[CrossRef](#)]
25. Corine Land Cover (CLC). Version 2020_20u1 Datasets. European Environment Agency (EEA) under the Framework of the Copernicus Program. 2012. Available online: <http://land.copernicus.eu/pan-european/corine-land-cover/clc-2012/view> (accessed on 10 June 2019).
26. Linke, S.; Lehner, B.; Dallaire, C.O.; Ariwi, J.; Grill, G.; Anand, M.; Beames, P.; Levine, V.B.; Maxwell, S.; Moidu, H.; et al. Global hydro-environmental sub-basin and river reach characteristics at high spatial resolution. *Sci. Data* **2019**, *6*, 283. [[CrossRef](#)]
27. Krug, J.A.; Wrather, W.E.; Langbein, W.B. Topographic characteristics of drainage basins. *Water Supply Pap.* **1947**, 125–157. [[CrossRef](#)]
28. Gravelius, H. *Grundrifi Grundriss der gesamten Gewässerkunde*; Band I: Flussfikunde (Compendium of Hydrology. Rivers, in German); Goschen: Berlin, Germany, 1914; Volume I.
29. Nautiyal, M.D. Morphometric analysis of a drainage basin using aerial photographs: A case study of Khairkuli basin, district Dehradun, U.P. *J. Indian Soc. Remote Sens.* **1994**, *22*, 251–261. [[CrossRef](#)]
30. Strahler, A.N. Quantitative Geomorphology of Drainage Basin and Channel Networks. Handbook of Applied Hydrology. 1964. Available online: <https://ci.nii.ac.jp/naid/10021229789/#cit> (accessed on 15 July 2019).
31. Chopra, R.; Dhiman, R.D.; Sharma, P.K. Morphometric analysis of sub-watersheds in Gurdaspur district, Punjab using remote sensing and GIS techniques. *J. Indian Soc. Remote Sens.* **2005**, *33*, 531–539. [[CrossRef](#)]
32. Christophe, B.; Louis-Daniel, P. Dealing with Logs and Zeros in Regression Models. Série des Documents de Travail n° 2019-13. 2020. Available online: <https://ssrn.com/abstract=3444996> (accessed on 28 August 2019).
33. Myronidis, D.; Ivanova, E. Generating Regional Models for Estimating the Peak Flows and Environmental Flows Magnitude for the Bulgarian-Greek Rhodope Mountain Range Torrential Watersheds. *Water* **2020**, *12*, 784. [[CrossRef](#)]
34. Kutner, M.; Nachtsheim, C.; Neter, J.; Li, W. *Applied Linear Statistical Models*; McGraw-Hill: New York, NY, USA, 2004.

35. Chatterjee, S.; Hadi, A.S.; Price, B. *The Use of Regression Analysis by Example*; John Wiley and Sons: New York, NY, USA, 2000.
36. Ahearn, D.S.; Sheibley, R.W.; Dahlgren, R.A.; Anderson, M.; Johnson, J.; Tate, K.W. Land use and land cover influence on water quality in the last free-flowing river draining the western Sierra Nevada, California. *J. Hydrol.* **2005**, *313*, 234–247. [[CrossRef](#)]
37. Amiri, J.B. *Environmental Modeling*, 2nd ed.; University Press, University of Tehran: Tehran, Iran, 2020; 150p.
38. Dawson, C.; Abrahart, R.; See, L. HydroTest: A web-based toolbox of evaluation metrics for the standardised assessment of hydrological forecasts. *Environ. Model. Softw.* **2007**, *22*, 1034–1052. [[CrossRef](#)]
39. Johnson, J.B.; Omland, K.S. Model selection in ecology and evolution. *Trends Ecol. Evol.* **2004**, *19*, 101–108. [[CrossRef](#)]
40. Burnham, K.P.; Anderson, D.R. Multimodel Inference: Understanding AIC and BIC in Model Selection. *Sociol. Methods Res.* **2004**, *33*, 261–304. [[CrossRef](#)]
41. Zhao, B.; Zhang, L.; Xia, Z.; Xu, W.; Xia, L.; Liang, Y.; Xia, D. Effects of Rainfall Intensity and Vegetation Cover on Erosion Characteristics of a Soil Containing Rock Fragments Slope. *Adv. Civ. Eng.* **2019**, *2019*, 1–14. [[CrossRef](#)]
42. Wu, Y.; Ouyang, W.; Hao, Z.; Lin, C.; Liu, H.; Wang, Y. Assessment of soil erosion characteristics in response to temperature and precipitation in a freeze-thaw watershed. *Geoderma* **2018**, *328*, 56–65. [[CrossRef](#)]
43. Mohamadi, M.A.; Kaviani, A. Effects of rainfall patterns on runoff and soil erosion in field plots. *Int. Soil Water Conserv. Res.* **2015**, *3*, 273–281. [[CrossRef](#)]
44. Egashira, K.; Tsuda, S.; Takuma, K. Relation between Soil Properties and the Erodibility of Masa Soils (Granitic Soils). *Soil Sci. Plant Nutr.* **1985**, *31*, 105–111. [[CrossRef](#)]
45. Tucker, G.; Bras, R.L. Hillslope processes, drainage density, and landscape morphology. *Water Resour. Res.* **1998**, *34*, 2751–2764. [[CrossRef](#)]
46. Clubb, F.J.; Mudd, S.M.; Attal, M.; Milodowski, D.T.; Grieve, S.W. The relationship between drainage density, erosion rate, and hilltop curvature: Implications for sediment transport processes. *J. Geophys. Res. Earth Surf.* **2016**, *121*, 1724–1745. [[CrossRef](#)]
47. Liu, Q.-Q.; Chen, L.; Li, J.-C. Influences of Slope Gradient on Soil Erosion. *Appl. Math. Mech.* **2001**, *22*, 510–519. [[CrossRef](#)]